Lab on a Chip

Cite this: *Lab Chip*, 2011, **11**, 1620

www.rsc.org/loc

PAPER

High sensitive matrix-free mass spectrometry analysis of peptides using silicon nanowires-based digital microfluidic device†

Florian Lapierre,[a] Gaëlle Piret,[b] Hervé Drobecq,[c] Oleg Melnyk,[c] Yannick Coffinier,[b] Vincent Thomy*[a] and Rabah Boukherroub*[b]

Received 21st December 2010, Accepted 18th February 2011
DOI: 10.1039/c0lc00716a

We present for the first time an electrowetting on dielectric (EWOD) microfluidic system coupled to a surface-assisted laser desorption–ionization (SALDI) silicon nanowire-based interface for mass spectrometry (MS) analysis of small biomolecules. Here, the transfer of analytes has been achieved on specific locations on the SALDI interface followed by their subsequent mass spectrometry analysis without the use of an organic matrix. To achieve this purpose, a device comprising a digital microfluidic system and a patterned superhydrophobic/superhydrophilic silicon nanowire interface was developed. The digital microfluidic system serves for the displacement of the droplets containing analytes, *via* an electrowetting actuation, inside the superhydrophilic patterns. The nanostructured silicon interface acts as an inorganic target for matrix-free laser desorption–ionization mass spectrometry analysis of the dried analytes. The proposed device can be easily used to realize several basic operations of a Lab-on-Chip such as analyte displacement and rinsing prior to MS analysis. We have demonstrated that the analysis of low molecular weight compounds (700 *m*/*z*) can be achieved with a very high sensitivity (down to 10 fmol μL^{-1}).

1 Introduction

Microfluidic devices have become widespread tools in several domains, notably due to the rapid development of technological processes in microelectronics. Silicon, glass, and more recently polymer-based microsystems, can rapidly be realized at non prohibitive time and price. Thus, this progress has provided very efficient tools to pluridisciplinary research groups for designing Lab-on-Chip devices dedicated to biochemical applications.[1] Independently of the targeted application, two main strategies have been developed with the aim to improve the performance and throughput: on chip integration of a novel detection system or coupling the microsystem to a pre-existing macroscopic detection/analysis device. Both approaches participate in the 'Holy Grail' quest (cheaper, faster, sensitive and multiplexed analysis of biochemical events) even though, most of the time, no universal system can fulfil all the requirements for biological applications such as enzyme assays, immunoassays,[2,3] DNA-based applications,[4,5] cell-based assays,[6] tissue engineering[7] and proteomics.[8,9]

Mass spectrometry (MS) is one of the most powerful techniques for real time control analysis of biomolecules such as proteins and peptides, including sequence and structure determinations, post-traductional modifications detection, quantification, and identification. MS has also found widespread applications in various fields such as forensics, terrorism (detection of explosives), petroleum and essential oils, atmospheric pollutants, *etc.*

Among the different techniques related to Digital MicroFluidic (DMF), electrowetting on dielectric (EWOD) is one the most widely used in Lab-on-Chip (LoC) applications dedicated to biomolecules analysis.[10–12] This phenomenon is now well depicted by the theoretical prediction made by Mugele *et al.*[13] EWOD relies on the modification of a liquid droplet–solid surface contact angle (CA) by application of an electrical potential between the droplet and the substrate. Under electrowetting at a microscopic scale, the CA is not modified, while the macroscopic CA of the droplet decreases.[14,15] To displace microdroplets and realize microfluidic basic operations (transporting, merging, creating droplets), the EWOD system is comprised of two parts: a hydrophobic base, consisting of an electrode network, and a conductive counter-electrode. When no voltage is applied between the electrodes and the counter-electrode, the initial CA of the drop is called θ_0. Upon application of a voltage, the CA of the three phase contact line, underneath the activated electrode, decreases to reach a value θ_V while the CA of the droplet placed on the un-activated electrode remains unchanged at θ_0. According to the Laplace law, the

[a]*IEMN, Avenue Poincaré, Villeneuve d'Ascq, France. E-mail: vincent.thomy@iemn.univ-lille1.fr; Fax: +03 20 19 78 80; Tel: +03 20 19 79 51*
[b]*IRI, Haute Borne, Université Lille Nord de France, France. E-mail: rabah.boukherroub@iri.univ-lille1.fr; Fax: +33 (0)3 62 53 17 01; Tel: +33 (0)3 62 53 17 24*
[c]*IBL, Institut de Biologie de Lille, Lille, France*
† Electronic Supplementary Information (ESI) available: See DOI: 10.1039/c0lc00716a/

meniscus curvature radius change involves a difference in pressure inside the drop leading to its displacement on the activated electrode. Up to this point all the calculations were made on perfect surfaces. However, certain forces such as hysteresis or viscous forces can hinder the displacement of a droplet. Therefore the driving force should be higher than the hysteresis force in order to displace a droplet. The use of a superhydrophobic surface as a counter-electrode clearly lowered the hysteresis force, compared to simple hydrophobic surfaces.[16]

Focusing on DMF and off-line MS analysis, Srinivasan *et al.*[17] succeeded for the first time to couple EWOD-DMF with matrix-assisted laser desorption/ionisation (MALDI)-MS analysis by moving protein sample droplets towards a stamping site where the analysis was performed (for bovine serum albumin (BSA) concentrations varying from 0.001 to 0.01 mg mL^{-1}). Wheeler's,[18–20] pioneering work in this field used EWOD-DMF to manipulate both organic matrices (for MALDI-MS) and biological liquid droplets. Once the biological droplets have been moved to the deposition sites, they were dried by a 1–2 min pause under vacuum. Impurities were then removed by water droplet displacement and finally droplets of the organic matrix were displaced and dried out (1–2 min in vacuum) on the deposition sites. Various operations (dispensing, merging and mixing) have been performed, showing that EWOD-DMF can be considered as a functional device for online sample preparation before MALDI-MS analysis. Protein processing has been realized on chip, including sample reduction, alkylation, digestion and co-crystallization with the matrix. Biological liquids tested contained angiotensin II and urea (0.3 μM and 100 mM respectively), insulin (1.75 μM, 0.0025% trifluoroacetic acid (TFA)), insulin chain B (2 μM, 0.025% TFA), cytochrom c (1.85 μM, 0.025% TFA), myoglobin (1.45 μM, 0.0125% TFA) with various matrices (2,5-dihydroxybenzoic acid (DHB), ferulic acid (FA) and sinapinic acid (SA)).

Nichols *et al.*[21] used a modified setup compared to the one developed by Wheeler *et al.* to investigate the pre-steady state reaction kinetics by combining rapid quenching and MALDI-MS analysis. They combined, with precise timing, four droplets' motion (creation, displacement and merging) to respectively initiate a reaction (0.5 μL of buffered 50 μM Yop51 PTPase and 20 mM *p*-nitrophenyl phosphate), quench it (1 M dichloroacetic acid) and then co-crystallize with FA for MS analysis. Furthermore, they used EWOD-DMF to create a micromixing inside the droplet and calibrated the mixing time according to the EWOD parameters (applied voltage and frequency).

More recently, C. J. Kim's group has demonstrated a new EWOD-DMF coupled with an off-line MALDI-MS analysis to incubate and digest proteins.[22] Their experiments showed that EWOD digital microfluidic chips can easily automate proteomics sample processing. Nonetheless, from these examples a few drawbacks can be underlined:

• As depicted in Table 1, the molecular weight (*m*/*z*) of the biomolecules analyzed using MALDI-MS–DMF coupled microsystems range from 1 to 6 kDa, with a minimum concentration of 0.33 nmol μL^{-1}, being the limit of detection of this technique.

• Microfluidic operations take at least 10 min before loading the chip into the MALDI-MS analyzer. This time is indubitably shorter than that necessary for the classical preparation of biological liquids, but is not negligible as compared to the few minutes (2 to 5 min) required for MALDI-MS analysis.

• Furthermore, the displacement of the organic matrix is not easy to realize due to its viscosity and composition (α-cyano-4-hydroxy-cinnamic acid, sinapinic acid, *etc.*). Another point concerns the homogeneity of the crystallization of analytes within the matrix that is essential to avoid the formation of hot spots and to reach optimal *D*/*I* and MS signal.

• The use of additives such as pluronic or oil films to reduce non-specific adsorption during the droplet motion can either lead to parasitic peaks, especially for high sensitive analysis, or reduce the liquid–surface interaction at the region of interest.

• Finally, analysis of low molecular weight compounds (<700 Da) such as peptides, carbohydrates or lipids is limited due to the strong background generated by the *D*/*I* of the organic matrix molecules.

Due to the matrix drawbacks listed above, a huge amount of work has been devoted to the development of matrix-free laser desorption–ionization techniques.[26] The first sensitive matrix-free desorption–ionization method on porous silicon, called DIOS-MS, has been proposed by Siuzdak *et al.*[27] In this technique, the sample to be analyzed is directly deposited on a chemically modified porous silicon substrate without addition of any organic matrix. Then, the spot is irradiated by a pulsed laser (same as in MALDI-MS). Emitted photons are absorbed by the porous layer and the energy is directly transferred to the sample. This transfer is assigned to the nanostructuration of the surface and a large number of rough surfaces have been successfully tested for matrix-free *D*/*I*-MS analysis.[28,29] We have recently shown that silicon nanowires, easily prepared *via* an electroless etching process, can be used as highly sensitive substrates for matrix-free LDI-MS.[30,31]

Tsao *et al.*[32] used dynamic electrowetting for effective target deposition on a silicon nanofilament for matrix-free LDI-MS analysis of proteins at the femtomolar level. However, to the best of our knowledge, there is no mention of a device combining EWOD sample actuation and matrix-free LDI-MS analysis.

In this paper, we present, for the first time, the integration of an off-line matrix-free LDI-MS analysis on silicon nanowires with a DMF system. The device comprises a patterned superhydrophobic/superhydrophilic silicon nanowire surface as a counter-electrode. The dimensions of the superhydrophilic area allow droplet displacement and transfer of a small amount of liquid for the analysis. The EWOD-DMF setup permits matrix-free MS analysis of a peptide mixture at a concentration down to 10 fmol μL^{-1}. The device displays several advantages:

• Concerning the droplet displacement, the use of a superhydrophobic surface (as a counter-electrode) reduces the drag friction, leading to low voltage displacement and self-cleaning properties, thus limiting non-specific adsorption of biomolecules along the droplet pathway.[33,34]

• Secondly, using an inorganic matrix such as silicon nanowires simplifies the analysis procedure. Indeed, no organic matrix is displaced and mixed with the analytes, avoiding the crystallization problem.

• Finally, small molecules can be analyzed (due to the absence of organic matrix molecules) with high sensitivity (fmol μL^{-1} level), not reached, to date, by a DMF–MALDI-MS device.

Table 1 EWOD-DMF–MALDI-MS devices described in the literature and their performances in terms of limit of detection

Peptides/proteins	Concentration	Authors[ref], year
Angiotensin II (m/z = 1046 Da)	1 pmol μL^{-1}	Wheeler *et al.*[23], 2006
Insulin chain B (m/z = 3495 Da)	1.75 pmol μL^{-1}	
Insulin (m/z = 5733 Da)	2 pmol μL^{-1}	
Cytochrom c (m/z = 12.4 kDa)	1.85 pmol μL^{-1}	
Myoglobin (m/z = 16.9 kDa)	1.45 pmol μL^{-1}	
Lys-C digests of equine myoglobin fragments (m/z = 1815, 2858, 1379, 1853, 1884, 1502, 1360)	2 pmol μL^{-1}	
Lys-C digests of bovine ubiquitin fragments (m/z = 1787, 1668, 1779, 1450)	2 pmol μL^{-1}	
Enzyme–substrate system: Yop51 PTPase *p*-Nitrophenyl phosphate	50 pmol μL^{-1} 20 nmol μL^{-1}	Nichols *et al.*[25], 2007
DNA Oligonucleotide (m/z = 6135 Da)	2.5 pmol μL^{-1}	Abdelgawad *et al.*[24], 2008
Angiotensin I (m/z = 1296.5 Da)	10 pmol μL^{-1}	Yang *et al.*[25], 2009
Angiotensin II (m/z = 1046 Da)	1 pmol μL^{-1}	
Insulin (m/z = 5733 Da)	35 pmol μL^{-1}	
Bradykinin (m/z = 1060 Da)	10 pmol μL^{-1}	
Oligonucleotide (m/z = 6135 Da)	10 pmol μL^{-1}	

2 Materials and methods

2.1 Reagents and materials

To realize the EWOD-DMF Lab-on-Chip system and silicon nanowire substrates, clean room reagents including AZnLOF2070, AZ4562 and SU-8 2002 photoresist, MIF-326 and SU-8 developers from MicroChemicals (Deutschland), hydrophobic Cytop from AGCE (Japan), glass substrates from ACM Verre Industrie (France), and p-type <100> crystalline highly doped silicon substrates (0.009–0.01 Ω cm^{-1}) from Siltronix (France), were used. Solid nickel deposition was performed on a PLASSYS MP 400S (France). Octadecyltrichlorosilane (OTS) was obtained from ABCR (Deutschland). Concentrated sulfuric acid (96%), hydrofluoric acid (50%) and hydrogen peroxide (30%) were all purchased from Carlo Erba. Nitric acid (65%), and hydrochloric acid (37%) were purchased from Merck. Silver nitrate (0.1 N), acetone isopropyl alcohol (*i*-PrOH), hexane and dichloromethane (CH_2Cl_2) were obtained from Sigma Aldrich.

2.2 Solution preparation

Piranha solution was prepared as a 3 : 1 (v/v) mixture of sulfuric acid and hydrogen peroxide. Silver nitrate and hydrofluoric acid solutions were respectively diluted 10 and 5 times before being mixed in proportions 1 : 1 (v/v). Cytop® solution was prepared by mixing Cytop® CTL-809M with its associated solvent CT-solv 180 (1 : 10, v/v). Safety considerations are available in the ESI.†

2.4 Sample preparation

A fluorescent 25 fmol μL^{-1} rhodamine-labeled peptide (lysine–arginine–tetramethylrhodamine (TMR)) solution was used to demonstrate the interaction between the liquid and the superhydrophilic areas created inside the superhydrophobic surface. For the LDI-MS analysis, a mixture of peptides Mix1 was obtained from a sequazyme peptide mass standard kit of Applied Biosystems (AB) (Part number P2-3143-00) and detailed in Table 2. It is to be noted that the neurotensin concentration is 5 times lower than the other peptides. The peptide solutions were then diluted in a 1 mM ammonium citrate aqueous solution to 50, 25 and 10 fmol μL^{-1} concentrations.

Table 2 Properties of the investigated peptides. The amino-acid colours in the peptide sequence correspond to (red) acidic residues, (blue) basic residues, (green) hydrophobic uncharged residues and (black) to other residues

Molecule	m/z	pI	Charges	Sequence	pH
Des-Arg-Bradykinin	904.5	10	1 (+)	PPGFSPFR	5.5
Angiotensin I	1296	7.4	2 (+)	DRVYIHPFHL	
Fibrinopeptide B	1570	4.0	3 (−)	EGVNDNEEGFFSAR	
Neurotensin	1672.9	8.7	1 (+)	ELYENKPRRPYIL	

2.5 LDI-MS characterisation

LDI-MS analysis was performed using a Voyager-DE-STR time-of-flight (ToF) mass spectrometer (Applied Biosystem) with delayed extraction, operating with a pulsed N_2 laser at 337 nm (3 ns pulse). Superhydrophobic cover substrates were attached to the usual MALDI-MS target using conductive double-side carbon tape. Positive ion mass spectra were acquired with a reflector mode of operation, an accelerating potential of 20 kV, and a grid voltage at 73%. Each spectrum is the result of 10 laser pulses.

2.6 Device fabrication and use

The base plate. EWOD-DMF devices were fabricated using a conventional clean room facility. First, the glass substrates were cleaned by a succession of acetone/isopropyl alcohol and piranha solution for 15 min. Then, a 20 nm thick nickel layer was deposited by evaporation and AZnLof2070 photoresist was

spin-coated (2700 rpm, 20 s). The resulting substrates were pre-baked on a hotplate (110 °C, 90 s) and then exposed to UV radiation (72 mJ cm^{-2}, 365 nm, 5.5 s) through a photomask using a Karl Suss MA6 mask aligner (Garching, Germany). After exposure, the substrates were post-baked (110 °C, 60 s) and developed in a MIF326 bath (90 s). The nickel was etched by a nitric acid aqueous solution (1 : 3, v/v) for 60 s, and then rinsed with deionized water. The remaining photoresist AZnLof2070 was stripped by a succession of acetone and isopropyl alcohol baths to reveal the electrodes.

A SU-8 2002 (2 μm thickness) dielectric layer was then spin-coated (4500 rpm, 30 s, 2 μm), pre-baked (95 °C, 60 s), exposed (80 mJ cm^{-2}, 365 nm, 6 s), post-baked (95°, 120 s), and developed in a SU-8 developer bath (60 s). Electrical contacts are SU-8 free to facilitate voltage supply towards the electrodes. Finally, a 30 nm thick hydrophobic layer of cytop® was spin-coated (1500 rpm, 30 s) and baked for 30 min at 180 °C. Contact angle and contact angle hysteresis are 112° and 12°, respectively (goniometer from Krüss GmbH, Deutschland).

The cover plate. The cover electrode consists of a highly doped silicon substrate. First, the silicon wafer was degreased in acetone and isopropyl alcohol, rinsed with deionized water and then cleaned in a piranha solution (3 : 1, v/v concentrated H_2SO_4–30% H_2O_2) for 20 min at 80 °C, followed by copious rinsing with Milli-Q water. The clean substrate was immersed in a HF (5% *i.e.* 2.625 M)–$AgNO_3$(0.005 M) aqueous solution at 54 °C for 30 min. The resulting surface was rinsed copiously with deionized water and immersed in an aqueous solution of HCl–HNO_3–H_2O (1 : 1 : 1, v/v/v) at room temperature overnight to remove the silver nanoparticles and dendrites deposited during the chemical etching. The nanowire diameters are in the range of 10–200 nm, and are 1 μm in height, as shown by the cross-sectional SEM view Fig. 1b.

To achieve the superhydrophobicity, the silicon nanowire surface was chemically modified with an OTS layer. First, the substrate was UV/ozone-treated (UV O Cleaner, Jelight Company, Inc., 4 mW cm^{-2} at 220 nm) for 30 min to remove any organic contaminants on the surface and to generate surface hydroxyl groups. The surface was then reacted with a 10^{-3} M OTS solution in hexane for 4 h at room temperature in a dry nitrogen purged glovebox. The resulting surface was rinsed with CH_2Cl_2, *i*-PrOH and dried under a gentle stream of nitrogen.[35–38] The contact angle and contact angle hysteresis are 164° and 1° respectively leading to a superhydrophobic character.

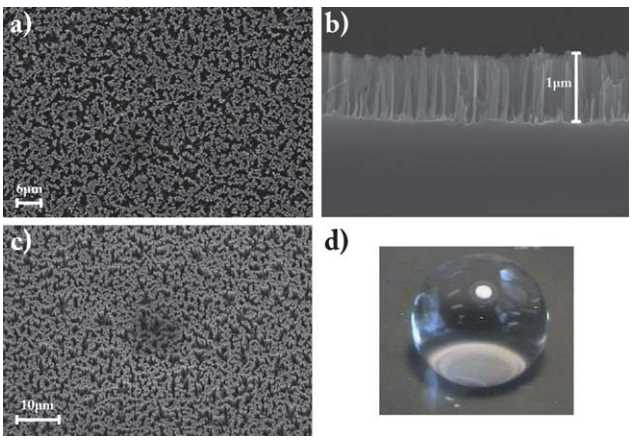

Fig. 1 SEM pictures of silicon nanowire substrate prepared by chemical etching of Si (100) in HF–$AgNO_3$ aqueous solution. (a) Top view, (b) cross view; the nanowire height is estimated to be 1 μm, (c) 30.5° tilted view, (d) picture of a spherical water droplet deposited on the superhydrophobic nanostructured surface.

Superhydrophilic patterns on the cover plate. To allow analyte deposition on localized plots, AZ4562 was spin-coated (2000 rpm, 10 s) on the superhydrophobic SiNWs surface, pre-baked (110 °C, 60 s), exposed (72 mJ cm^{-2}, 365 nm, 5.5 s) through an optical mask, post-baked (110 °C, 60 s) and developed in a MIF-326 bath (90 s). Then, an oxygen plasma (100 W, 100 mT, 20 sccm, 3 min) was performed to remove the OTS at the localized patterns. We denoted the inside zone or area the superhydrophilic patterns and the outside zone or area the superhydrophobic part of the cover plate.

EWOD-DMF. Droplet displacements by EWOD-DMF were carried out as follows: a LabView program multiplexes an electrical square voltage (100 V_{TRMS}, 1 kHz) to the 96 electrodes (4 mm^2 in size) controlling the droplet displacement. A Teflon holder encapsulates a 1 μL droplet between the superhydrophobic counter-electrode, connected to the ground, and the base electrode (Fig. 2a). The gap (300 μm) is set by a metallic spacer under the counter electrode. A video camera (JVC, 25 fps) records the droplet motion. The electrode network of the EWOD-DMF device allows all the microfluidic operations with the 1 μL droplets such as separation, transport and merging processes. The droplet speed is set by the LabView program at 100 mm s^{-1}. Thus, the droplet will be in contact with the superhydrophobic cover surface for 2 ms on each electrode. It is to be noted that the size of the superhydrophilic patterns on the cover plate are carefully selected. These areas have to be smaller than 250 μm to avoid droplet sticking but their size must to be larger than the laser spot diameter (about 100 μm) to achieve high efficiency LDI-MS analysis. Thus, water droplet actuation is possible with a superhydrophilic cover surface up to 2% of the droplet–nanowire interface (corresponding to a maximum of 4 areas of 150 μm diameter per 4 mm^2). Knowing that the liquid to be tested by LDI-MS presents a higher wettability than water, only 1% of the surface has been chosen for a better EWOD displacement reproducibility. Thus, the optimal dimensions of the superhydrophilic areas are a 100 μm side spaced by 4000 μm.

The experimental protocol is as follows:

• A 1 μL droplet of the peptide mixture is deposited on the base and encapsulated with a Teflon holder. The droplet is displaced on 8 electrodes and then removed from the base. During the droplet actuation, a small amount of the solution is adsorbed on the superhydrophilic areas (Fig. 2b).

• Depending on the protocol (rinsing step or not), a deionized water droplet is displaced along the same path at the same speed, simulating the true operations (deposition of sample, rinsing step, *etc.*) occurring in a lab-on-chip device.

It is to be noted that the system is opened in order to remove the droplet and to perform off-line LDI-MS analysis (see Fig. S1†).

Validation of the superhydrophilic pattern. Prior to the realization of displacement of a droplet containing the peptide

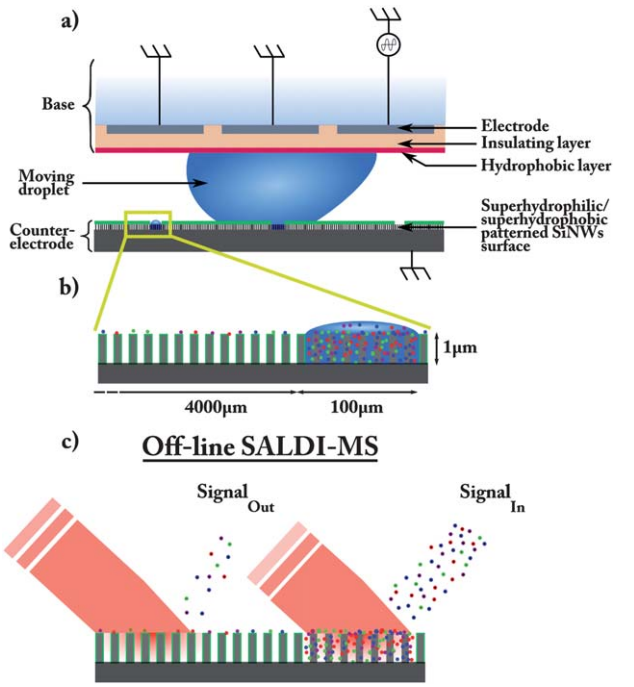

Fig. 2 (a) Schematic illustration of EWOD-DMF displacement using a network of electrodes. When the droplet is moved along the electrode path the liquid is confined inside the superhydrophilic areas (100 μm diameter, 4000 μm spaced). (b) Magnified view of liquid impregnation inside the superhydrophilic area. (c) LDI-MS analysis on the superhydrophobic silicon nanowire surface (S_{out}) and on the superhydrophilic silicon nanowire region (S_{in}).

mixture and their deposition inside the superhydrophilic areas followed by their subsequent mass spectrometry analysis, we first performed fluorescence measurements to validate the size of the patterns and the interaction of the liquid droplet containing the analytes. A 1 μL droplet of rhodamine-labeled peptide (Lysine–Arginine–Rhodamine, 25 fmol μL^{-1}) was displaced following the experimental protocol without a rinsing step. Fig. 3 shows the fluorescence image obtained after displacement of a 1 μL droplet containing the rhodamine-labeled peptide (25 fmol μL^{-1}) on a patterned superhydrophilic/superhydrophobic surface.

We estimate the nanodroplet volume inside each superhydrophilic pattern to be higher than 10 pL by maximizing the volume (100 $\mu m^2 \times 1$ μm).

To conclude, the transfer of a fluorescently-labeled peptide is very effective from the droplet to the superhydrophilic areas. Moreover, a very low level of fluorescence intensity on the superhydrophobic surface was observed for an interaction time as low as 2 ms, suggesting a low level of non-specific adsorption.‡

EWOD–LDI-MS experiments. The same protocol has been performed using a 1 μL droplet of a peptide mixture at different concentrations: 10, 25 and 50 fmol μL^{-1}. After each displacement, the peptides trapped inside the superhydrophilic patterns and on the superhydrophobic silicon nanowire surfaces are characterized by LDI-MS. Signal-to-Noise (S/N) values were calculated for each peptide and for each superhydrophilic pattern corresponding to 5 patterns per surface. Then, the ratio of S/N_{in} and S/N_{out} (Fig. 2c) were calculated giving the average of the S/N of [Des-Arg1]-bradykinin ($m/z = 904.5$ Da) inside (5 spectra) and outside, 5 superhydrophilic patterns, respectively. At least 3 experiments were performed for each concentration.

‡ Lower droplet motions (from 2 to 100 mm s^{-1}) were also investigated. However in this paper, we only discuss the optimal results obtained for the highest speed where the lowest non-specific adsorption on the superhydrophobic region was observed.

3 Results and discussion

3.1 LDI-MS analysis without a rinsing step

MS spectra have been performed after EWOD displacement of a droplet of Mix1 (25 fmol μL^{-1}) at 100 mm s^{-1} along the cover surface inside and outside a superhydrophilic pattern. Fig. 4a shows one spectrum obtained from one superhydrophilic pattern and Fig. 4b on the surrounding superhydrophobic surface.

From the obtained mass spectra, one clearly sees a difference in terms of signal intensities, signal to noise (S/N) ratio and detected peptides for each zone. Indeed, the S/N ratio of the [Des-Arg1]-bradykinin (m/z = 904.5 Da) peak is 460 for a superhydrophilic pattern compared to 223, *i.e.* 2 times lower, for the superhydrophobic surface. Similarly for angiotensin I ($m/z = 1296$ Da), the signal intensity is also two times lower on the superhydrophobic surface (S/N_{out} = 226) than on the superhydrophilic regions (S/N_{in} = 430). Finally, concerning the [Glu1]-fibrinopeptide B ($m/z = 1570$ Da) and neurotensin (m/z = 1672.9 Da) peaks, they are barely visible inside and outside the patterns.

First, the S/N values depend on the peptides' D/I which is related to their inherent physico-chemical properties such as pI, hydrophobicity, hydrophilicity, number of charges and their concentration (summarized in the Table 2).

Due to its pI and to the sample pH (5.5), fibrinopeptide is the only negatively charged peptide. During the short contact time between the superhydrophilic pattern and the droplet, a higher amount of peptides that are positively charged adsorb specifically to the SiO_2 surface. Thus, a very weak interaction with the superhydrophilic apertures ($-SiO^-$) is expected and can explain its weak signal in the MS spectrum, compared to the other peptides (the neurotensin concentration in the mixture is 5 times lower than the other peptides). Moreover, the mass spectra are acquired in the positive ion mode, reducing the detection of this peptide.[30,39]

Nevertheless, interactions of peptides within the superhydrophilic area are different with regards to their amino acid sequence. Indeed, Willett *et al.*[40] have demonstrated that amino acid residues can have different adhesion properties to inorganic interfaces such as SiO_2, Si_3N_4, metals, essentially depending on their side chains. They found that E (Glu) has better adhesion to SiO_2 than His (H) > Lys(K) > Arg(R) > Asp(D) > Thr(**T**) > Pro (**P**), and that other amino acid residues have very weak adhesion on such an interface. In addition, Goede *et al.*[41] have shown that the peptidic sequence could have also an influence on the peptide adhesion on semiconducting interfaces.

For the present study, EWOD-DMF allowed the deposition of sample nanodroplets inside the superhydrophilic patterns, their penetration inside the nanostructures and sample concentration inside these patterns. Concerning the superhydrophobic

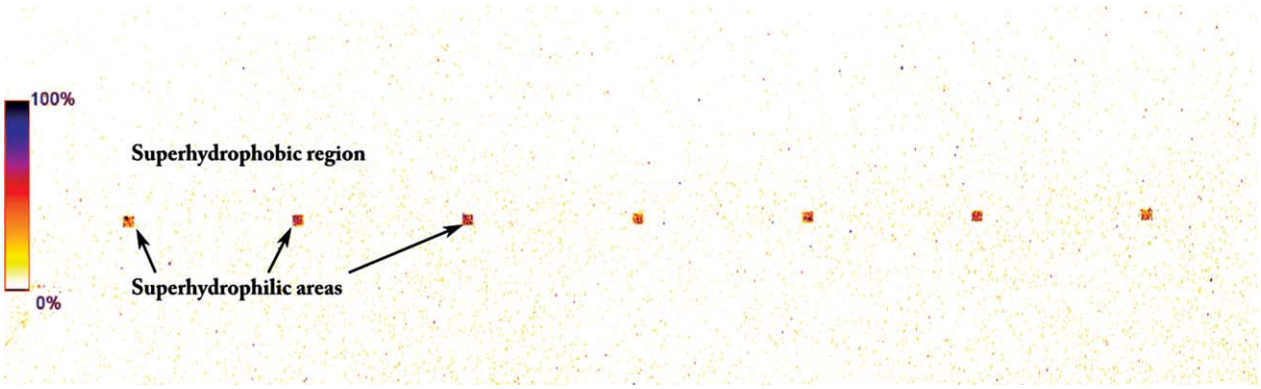

Fig. 3 Fluorescence image of the patterned superhydrophilic/superhydrophobic surface after displacement of a 1 μL rhodamine-labeled peptide (25 fmol μL^{-1}) droplet by EWOD-DMF (100 mm s^{-1} – 100 V_{TRMS}). The fluorescence is only visible inside the superhydrophilic patterns (100 μm size, spaced by 4000 μm). The image has been artificially colored to improve clarity.

surrounding areas, the droplet of sample has a small contact area with the surface and the MS signal intensity recorded in these areas is two times lower than that inside the superhydrophilic ones. However, the result also suggests that a non-neglectable, non-specific adsorption outside the apertures takes place. A short contact time between the droplet and the superhydrophobic zone seems to be enough for the deposition of peptides. These observations had already been reported by Trauger *et al.*[28] during the deposition and removal of a microdroplet containing a mixture of peptides on different superhydrophobic surfaces. Their MS results showed the presence of peptides, demonstrating both the deposition of peptides (even with a short time of contact with the surface) and high sensitivity of these specific surfaces.

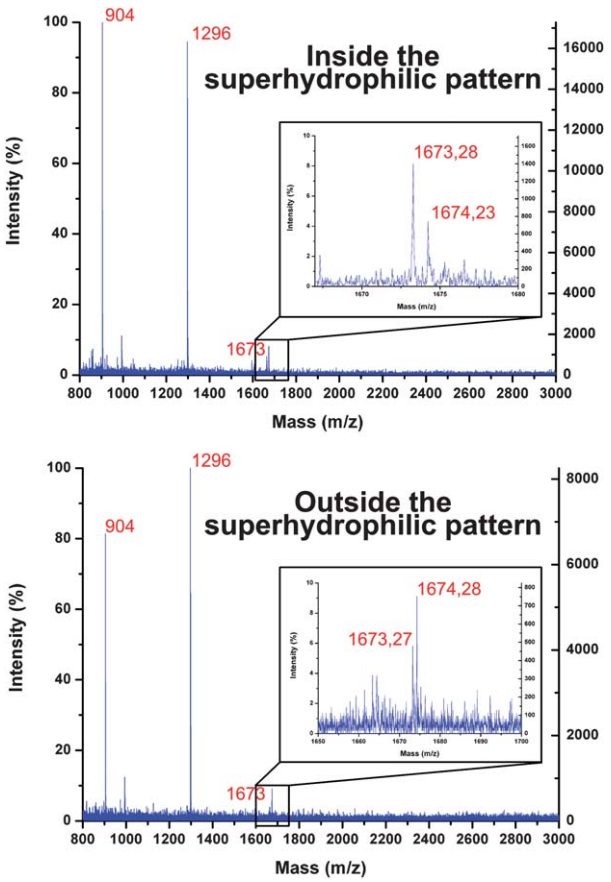

Fig. 4 Mass spectra after 1 EWOD displacement of 1 μL of Mix1 (25 fmol μL^{-1}) over 5 patterns recorded inside (a) and outside a superhydrophilic pattern (b). No rinsing step was performed.

3.2 LDI-MS analysis with a rinsing step

Fig. 5 displays the LDI-MS spectra for the same experiment as above, except that a rinsing step with a droplet of deionized water was performed just after the sample displacement with the same EWOD-DMF. Compared to the spectra obtained without rinsing, the signal intensity is 50% higher inside the superhydrophilic areas, and about 10 times lower outside the apertures. Furthermore, compared to the previous spectra without rinsing, all peptides are detected, even those present at a low concentration. It is to be noticed that the angiotensin I (m/z = 1296 Da) peak in Fig. 5a is reduced compared to the one in Fig. 4a. The rinsing step has most likely removed some of this peptide inside the superhydrophilic patterns.

This can be ascribed to the self-cleaning property of the surface. Indeed, a water droplet can remove an important amount of the peptides adsorbed on the superhydrophobic surface. The collected peptides are most likely re-deposited inside the superhydrophilic areas, enhancing the MS signal. To illustrate the self-cleaning properties of superhydrophobic surfaces, Koc *et al.*[34] have shown that a similar amount of ovalbumin adsorbs onto smooth (hydrophobic) and rough (superhydrophobic) nanometre-scale surfaces. After a cleaning step, they removed a larger amount of adsorbed proteins from the superhydrophobic surfaces than from the smooth ones, with almost all the tested proteins being removed from the nanoscale superhydrophobic surface.§ In our case, the contact between the tested peptides and the superhydrophobic surface is dramatically reduced. Then, during the displacement of the water droplet, peptides are easily collected. This self-cleaning property has also been pointed out by Lapierre *et al.*[16] with different bio-particles

§ It is to be noted that the cleaning efficiency and the D/I will depend of the properties of each peptide.

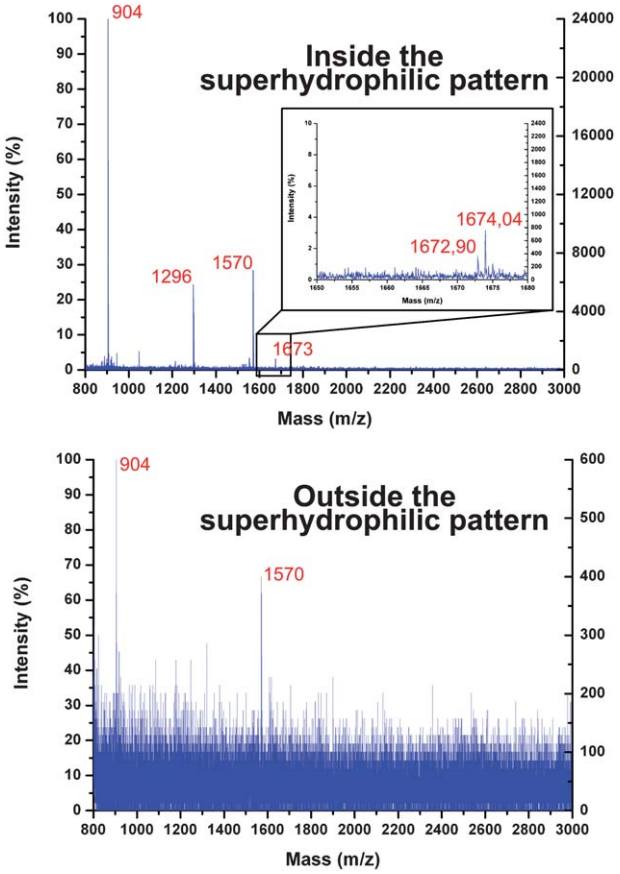

Fig. 5 Mass spectra of a peptide mixture (25 fmol μL^{-1}) deposited after 1 displacement by EWOD on 5 electrodes, (a) inside the superhydrophilic patterns and (b) on the superhydrophobic surface. A rinsing step with deionized water was performed after the sample deposition. The interaction time of the droplet mixture with the superhydrophilic pattern is set at 2 ms. Signal inside the pattern is strong with a S/N_{in} equal to 864 for the [Des-Arg1]-bradykinin (m/z = 904.5 Da).

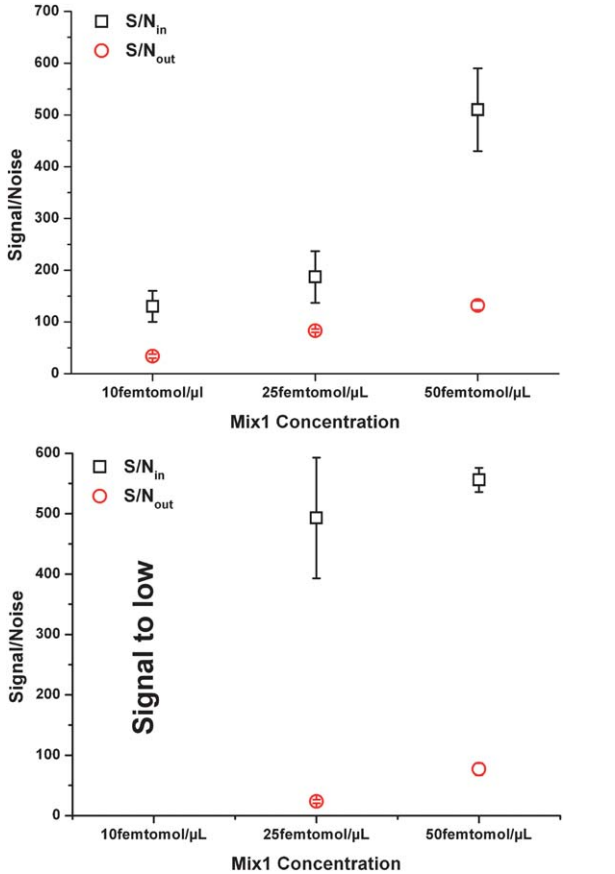

Fig. 6 (a) S/N inside (black dots) and outside (reds dots) for the [Des-Arg1]-bradykinin (m/z = 904.5 Da) peptide at 10, 25 and 50 fmol μL^{-1}. No rinsing step was performed after the sample displacement. (b) A rinsing step was performed after the sample displacement.

(proteins, spores and phages). After one displacement of a water droplet, proteins such as ovalbumin are totally removed from the superhydrophobic surface with more than 90% efficiency.

These results are confirmed by the S/N ratios calculated between the superhydrophobic surface and the superhydrophilic area. In Fig. 6, are displayed the evolution of the S/N for Des-Arg1-bradykinin peptide at different concentrations (10, 25 and 50 fmol μL^{-1}) from MS spectra without (a) and with (b) a rinsing step. We deliberately realized all measurements on this peptide as it always shows the highest S/N ratio. Red dots correspond to the average S/N outside the superhydrophilic regions (S/N_{out}), and black dots to the ones calculated inside the superhydrophilic spots (S/N_{in}).

On Fig. 6a, one can clearly see an increase of S/N as a function of Des-Arg1-bradykinin concentration in the superhydrophilic regions as compared to the superhydrophobic one, where only a slight increase is observed. This enhancement is more significant for a concentration of 50 fmol μL^{-1}, suggesting that a higher amount of peptides is deposited. For all the three concentrations, the S/N values obtained on the superhydrophobic surface have a small error bar, suggesting that the amount of the deposited peptides is uniform on the overall superhydrophobic surface surrounding the superhydrophilic patterns. On the other hand, the error bar for each superhydrophilic pattern for all concentrations is higher, indicating that different amounts of peptides were deposited. In this case, it is believed that the peptides have penetrated the overall superhydrophilic structure of the silicon nanowires leading to a non-uniform distribution from the top to the bottom part of the wires for each superhydrophilic pattern. The laser ionized different amounts of peptides in each superhydrophilic area, generating different MS signals. On the superhydrophobic surface, a droplet stays in a Cassie–Baxter state, *i.e.* the droplet containing the peptides did not penetrate the silicon nanowire network and remained on the top of the surface. The laser spot "hits" relatively the same amount of peptides leading to comparable mass spectrometry signals.

Fig. 6b shows S/N outside and inside the superhydrophilic patterns for different Des-Arg1-bradykinin concentrations after a single rinsing step with a deionized water droplet. A slight decrease of S/N_{out} (23 and 77 for 25 and 50 fmol μL^{-1}, respectively) was observed, resulting in the removal of adsorbed peptides on the superhydrophobic region. In this figure, the most significant change is the strong increase of the S/N_{in} for the 25 fmol μL^{-1} concentration. Indeed, a S/N_{in} of 493 was calculated, which is 2.6 times higher than that obtained without a rinsing step and close to that estimated for 50 fmol μL^{-1}. After rinsing, the ratio between the S/N ratio calculated on the superhydrophilic patterns and superhydrophobic regions is

increased by 10 times, indicating the efficiency of the rinsing step. These results are consistent with the fact that adsorbed peptides on the superhydrophobic surface are most likely re-suspended in the water droplet and then re-adsorbed onto the superhydrophilic areas.

For a concentration of 10 fmol μL^{-1}, only traces of peptides were detected even after a rinsing step with deionized water. The displacement of a water droplet may have removed most of the physisorbed peptides or it is possible that the peptides are diluted in the rinsing water droplet and inhomogeneously redeposited in the superhydrophilic micropatterns. In the same way, regarding the error bar for the 25 fmol μL^{-1}, one can deduce that the re-adsorption is not uniform over all the superhydrophilic patterns due to different amounts of peptides being transferred from outside to inside regions.

Finally, one can argue that this is not a real rinsing step but a peptide deposition occurring in two steps.

4 Conclusion

EWOD-DMF systems have proved their efficiency for Lab-on-Chip applications, particularly concerning their easy integration into a MALDI-MS analysis system. The use of a super-hydrophobic silicon nanowire cover surface in a digital micro-fluidic system as a counter-electrode and as inorganic target for matrix-free LDI-MS analysis led to an easy to handle MS analysis procedure. Furthermore, the realization of superhydrophilic micropatterns in the superhydrophobic surface permits to locate and concentrate a small amount of liquid containing biomolecules. For a concentration of 25 fmol μL^{-1} peptides were detected with a high *S*/*N* ratio after only one short (2 ms) displacement over the superhydrophilic apertures. We have shown that a rinsing step with deionized water allowed an enhancement of the *S*/*N* ratio *via* a re-suspension–re-deposition step. However, for a concentration of 10 fmol μL^{-1} only traces of peptides were detected, even after a rinsing step. This could most likely be due to the resolution of the mass spectrometer. The proposed microfluidics protocol allows a highly simplified sample deposition, taking place in less than 2 s. This proof of concept of a rapid, easy to handle and highly sensitive MS analysis technique for Lab-on-Chip has now to be pursued. To reach a lower limit of detection, EWOD could be used to induce micromixing, enhance the mass transfer toward the superhydrophilic areas. Furthermore, to improve the device performance, we can introduce a high level of selectivity and thus a specific recognition toward biological targets: *i.e.* selecting one specific biomolecule among complex biological fluids *via* an appropriate surface chemistry inside the apertures. Finally, we can also take advantage of the device performance to use it for classical fluorescence detection of biomolecular interactions. The use of super-hydrophobic silicon nanowire interfaces with superhydrophilic apertures presented weak non-specific adsorption outside the apertures. From this, we can consider that our device could be useful for the fluorescence detection of antigen–antibody or DNA–DNA interactions, *etc.*

5 Acknowledgements

The European Community's Seventh Frame-work Programme (FP7/20072013) under grant agreement no. 227243 and the Centre National de la Recherche Scientifique (CNRS) are gratefully acknowledged for financial support.

References

1 H. Becker, *Lab Chip*, 2009, **9**, 2119–2122.
2 R. Sista, Z. Hua, P. Thwar, A. Sudarsan, V. Srinivasan, A. Eckhardt, M. Pollack and V. Pamula, *Lab Chip*, 2008, **8**, 2091–2104.
3 R. S. Sista, A. E. Eckhardt, V. Srinivasan, M. G. Pollack, S. Palanki and V. K. Pamula, *Lab Chip*, 2008, **8**, 2188–2196.
4 Y.-H. Chang, G.-B. Lee, F.-C. Huang, Y.-Y. Chen and J.-L. Lin, *Biomed. Microdevices*, 2006, **8**, 215–225.
5 Z. Hua, J. L. Rouse, A. E. Eckhardt, V. Srinivasan, V. K. Pamula, W. A. Schell, J. L. Benton, T. G. Mitchell and M. G. Pollack, *Anal. Chem.*, 2010, **82**, 2310–2316.
6 I. Barbulovic-Nad, H. Yang, P. S. Park and A. R. Wheeler, *Lab Chip*, 2008, **8**, 519–526.
7 J. Zhou, L. Lu, K. Byrapogu, D. M. Wootton, P. I. Lelkes and R. Fair, *Virtual Phys. Prototyping*, 2007, **2**, 217223.
8 V. N. Luk, G. C. Mo and A. R. Wheeler, *Langmuir*, 2008, **24**, 6382–6389.
9 H. Moon, A. Wheeler, R. Garrell, J. Loo and C.-J. Kim, *Micro Electro Mech. Syst., IEEE Int. Conf., 18th*, 2005, 859–862.
10 Z. Guttenberg, H. Muller, H. Habermuller, A. Geisbauer, J. Pipper, J. Felbel, M. Kielpinski, J. Scriba and A. Wixforth, *Lab Chip*, 2005, **5**, 308–317.
11 L. Malic, T. Veres and M. Tabrizian, *Biosens. Bioelectron.*, 2009, **24**, 2218–2224.
12 L. Malic, D. Brassard, T. Veres and M. Tabrizian, *Lab Chip*, 2010, **10**, 418–431.
13 F. Mugele and J.-C. Baret, *J. Phys.: Condens. Matter*, 2005, **17**, R705–R774.
14 F. Mugele and J. Buehrle, *J. Phys.: Condens. Matter*, 2007, **19**, 375112–375132.
15 F. Lapierre, P. Brunet, Y. Coffinier, V. Thomy, R. Blossey and R. Boukherroub, *Faraday Discuss.*, 2010, **146**, 125–139.
16 M. Jonsson-Niedziolka, F. Lapierre, Y. Coffinier, S. J. Parry, F. Zoueshtiagh, T. Foat, V. Thomy and R. Boukherroub, *Lab Chip*, 2011, **11**, 490–496.
17 V. Srinivasan, V. Pamula, P. Paik and R. Fair, *Lab-on-a-Chip: Platforms, Devices, and Applications*, 2004.
18 A. R. Wheeler, H. Moon, C.-J. C. Kim, J. A. Loo and R. L. Garrell, *Anal. Chem.*, 2004, **76**, 4833–4838.
19 A. R. Wheeler, H. Moon, C. A. Bird, R. R. Ogorzalek Loo, C.-J. C. Kim, J. A. Loo and R. L. Garrell, *Anal. Chem.*, 2005, **77**, 534–540.
20 M. J. Jebrail, A. H. C. Ng, V. Rai, R. Hili, A. K. Yudin and A. R. Wheeler, *Angew. Chem., Int. Ed.*, 2010, **49**, 8625–8629.
21 K. P. Nichols and J. G. E. Gardeniers, *Anal. Chem.*, 2007, **79**, 8699–8704.
22 W. C. Nelson, I. Peng, G.-A. Lee, J. A. Loo, R. L. Garrell and C.-J. Kim, *Anal. Chem.*, 2010, **82**, 9932–9937.
23 H. Moon, A. R. Wheeler, R. L. Garrell, J. A. Loo and C.-J. C. Kim, *Lab Chip*, 2006, **6**, 1213–1219.
24 M. Abdelgawad, S. L. S. Freire, H. Yang and A. R. Wheeler, *Lab Chip*, 2008, **8**, 672–677.
25 H. Yang, V. N. Luk, M. Abelgawad, I. Barbulovic-Nad and A. R. Wheeler, *Anal. Chem.*, 2009, **81**, 1061–1067.
26 D. S. Peterson, *Mass Spectrom. Rev.*, 2007, **26**, 19–34.
27 J. Wei, J. M. Buriak and G. Siuzdak, *Nature*, 1999, **399**, 243–246.
28 S. A. Trauger, E. P. Go, Z. Shen, J. V. Apon, B. J. Compton, E. S. P. Bouvier, M. G. Finn and G. Siuzdak, *Anal. Chem.*, 2004, **76**, 4484–4489.
29 T. R. Northen, O. Yanes, M. T. Northen, D. Marrinucci, W. Uritboonthai, J. Apon, S. L. Golledge, A. Nordstrom and G. Siuzdak, *Nature*, 2007, **449**, 1033–1036.
30 G. Piret, H. Drobecq, Y. Coffinier, O. Melnyk and R. Boukherroub, *Langmuir*, 2010, **26**, 1354–1361.
31 G. Piret, R. Desmet, E. Diesis, H. Drobecq, J. Segers, C. Rouanet, A.-S. Debrie, R. Boukherroub, C. Locht and O. Melnyk, *J. Proteome Res.*, 2010, **9**, 6467–6478.
32 C.-W. Tsao, P. Kumar, J. Liu and D. L. DeVoe, *Anal. Chem.*, 2008, **80**, 2973–2981.
33 G. McHale, M. I. Newton and N. J. Shirtcliffe, *Soft Matter*, 2010, **6**, 714–719.

34 Y. Koc, A. J. d. Mello, G. McHale, M. I. Newton, P. Roach and N. J. Shirtcliffe, *Lab Chip*, 2008, **8**, 582–586.
35 K. Peng, H. Fang, J. Hu, Y. Wu, J. Zhu, Y. Yan and S. Lee, *Chem.–Eur. J.*, 2006, **12**, 7942–7947.
36 Y. Coffinier, S. Janel, A. Addad, R. Blossey, L. Gengembre, E. Payen and R. Boukherroub, *Langmuir*, 2007, **23**, 1608–1611.
37 G. Piret, Y. Coffinier, C. Roux, O. Melnyk and R. Boukherroub, *Langmuir*, 2008, **24**, 1670–1672.
38 E. Galopin, G. Piret, S. Szunerits, Y. Lequette, C. Faille and R. Boukherroub, *Langmuir*, 2010, **26**, 3479–3484.
39 R. A. Kruse, X. Li, P. W. Bohn and J. V. Sweedler, *Anal. Chem.*, 2001, **73**, 3639–3645.
40 R. L. Willett, K. W. Baldwin, K. W. West and L. N. Pfeiffer, *Proc. Natl. Acad. Sci. U. S. A.*, 2005, **102**, 7817–7822.
41 K. Goede, P. Busch and M. Grundmann, *Nano Lett.*, 2004, **4**, 2115–2120.